Space Weather Applications of the UAF Eulerian Parallel Polar Ionosphere Model (EPPIM)

Sergei Maurits, Anton Kulchitsky
Arctic Region Supercomputing Center
University of Alaska Fairbanks
Fairbanks, Alaska 99775
USA

maurits@arsc.edu

Brenton Watkins
Geophysical Institute
University of Alaska Fairbanks
Fairbanks, Alaska 99775
USA

ABSTRACT

UAF EPPIM is the first principles theoretical model of the polar ionosphere, which covers region pole ward from 50ºN of geomagnetic latitude, and altitudes from 80 to 900-1000 km. If available, the model can input real data or, conversely, it is capable of generating all necessary inputs using statistical modules (e.g., MSIS, electric field, precipitation intensity, etc.) incorporated into the model and driven by the standard set of geophysical indices ($F_{10.7}$, Ap/Kp, IMF). UAF EPPIM is a computationally robust scaleable high-resolution model, capable of running on a range of platforms from desktop to a parallel supercomputer. Its real-time performance with useful resolution of 30x30x10 km or better can be achieved on a low-cost workstation. The model real-time continuous operation is arranged at the Arctic Region Supercomputing Center (ARSC) of the University of Alaska Fairbanks (UAF). It is based on automatic updates of the UAF EPPIM standard inputs (F10.7, Ap/Kp, and IMF), which are regularly fetched from the NOAA Space Environment Center (SEC) on-line depository. The solar wind IMF information from the upstream-located ACE satellite is available with advance of up to 2 hours, which facilitates forecasting mode of the ionospheric model. The model time is shifted forward to accommodate this time advance for the arriving solar wind. The forecast products in a number of formats are output in to the model WWW-site (http://www.arsc.edu/SpaceWeather) for immediate dissemination to the users and for past analysis and archiving. Statistical determination of the forecasting accuracy is performed by massive comparisons (>200,000 per year) with the NOAA SEC ionosonde data. The emulated critical frequency foF2 is automatically compared to the real-time data from about twenty sounding stations situated inside the model domain. The model statistical bias and RMS are determined on monthly basis for the daytime, twilights, and the night-time conditions. Such comparisons cover more than three-year period during current solar minimum, starting from September 2002 to present time. The collected archive demonstrates that RMS accuracies of the foF2 forecast are typically in the range of 10-20% (summer, daytime) to 20-40% (winter, night-time). It is shown that statistical bias is a convenient metrics for elimination of the systematic errors in the model. Empirical correction for the nighttime downward flux as a function of season and location for the upper boundary condition was performed to minimize the nighttime statistical bias. It resulted in reduction of the initial nighttime forecasting error by a factor of 2-3. This study demonstrates that ionospheric model of polar and adjacent mid-latitude region continuously operated with statistical inputs, which, in turn, are driven by the period-specific series of geophysical indices is capable of providing useful space weather forecasts. Further improvement of the forecasts by applying data assimilation techniques is discussed as future work.

Maurits, S.; Kulchitsky, A.; Watkins, B. (2006) Space Weather Applications of the UAF Eulerian Parallel Polar Ionosphere Model (EPPIM). In *Characterising the Ionosphere* (pp. 11-1 – 11-14). Meeting Proceedings RTO-MP-IST-056, Paper 11. Neuilly-sur-Seine, France: RTO. Available from: http://www.rto.nato.int/abstracts.asp.

1.0 INTRODUCTION

Application of theoretical models of ionosphere to the diagnostic and forecasting tasks is a filed of growing interest [Maurits et al., 2000; Wang et al., 2004; Schunk et al., 2004]. During the last decade advances of data-collection infrastructure and networking made it possible to generate geophysical data in real-time and to disseminate it to the users from on-line depositories such as NOAA Space Environment Center (SEC, http://www.sec.noaa.gov) and many others. Such readily available data as the solar activity index $F_{10.7}$; geomagnetic activity index *Kp/Ap*; the solar wind velocity, density, and the frozen Interplanetary Magnetic Filed (IMF) are sufficient for driving a number of statistical models, which, in turn, can generate all necessary inputs for the ionospheric simulations. For polar ionosphere, this list includes models of the spectral intensities of the solar Extreme Ultraviolet (EUV), models of the neutral thermosphere temperature and composition, neutral wind models, models of the magnetospheric electric field, and models of the auroral precipitations. Each of these "climatological" models is a statistical model by its nature, valid for the specified geophysical indices only on average. Application of such models for specification of geophysical conditions for particular date and time ("period-specific" conditions) by matching their geophysical drivers is possible only with a certain error. Elimination or, at least, reduction of such climatological input-induced errors is achievable with various data assimilation techniques. These methods aimed to facilitate a closer fit of simulations with the measured data. Effectively, a correction of simulation inputs to actual period-specific realization is performed by these techniques either directly (variation methods for period-specific correction of inputs) or indirectly (Gauss-Markov filtering of the outputs at each time step). Obviously, a measure of success of such methods is a reduction of overall error in the simulation scheme. Important question for quantitative determination of improvement here is a "ground level" of the simulation errors. It is comprised by typical errors of simulations performed with statistical (or climatological) inputs driven by the date-specific combinations of the geophysical indices. This effort targets determination of such errors both for assessment of the current level of the modeling accuracies of the polar ionosphere and for the future comparisons with the data-corrected schemes.

Since sensitivity of ionospheric model to uncertainties in different inputs varies and a theoretical model itself is not free of simplifications and hence its own errors, it appears that the only practical way to determine overall simulation error is a statistically valid comparison of the modeling results with the measurements. The key words here are "statistically valid", which implies massive number of comparisons performed during extended modeling period of at least model months or, much preferable, model years. The second requirement is availability of representative set of data covering more-or-less evenly the model simulation domain. These two criteria are met for continuous real-time run of the University of Alaska Eulerian Parallel Polar Ionosphere Model (UAF EPPIM), last three years worth of outputs of which is compared in this paper with the real-time ionosonde network data disseminated by the NOAA Space Environment Center.

2.0 UAF EPPIM (EULERIAN PARALLEL POLAR IONOSPHERE MODEL)

The UAF EPPIM (University of Alaska Fairbanks Eulerian Polar Parallel Ionospheric Model) [*Maurits and Watkins,* 1996] is the first principles three-dimensional time-dependent theoretical model. It solves equations of conservation of mass, momentum, and energy balance for electrons, seven ion species, and a few minor neutral components of odd nitrogen family, which are important for ionization balance of the lower ionosphere. The model equations are solved in geographic frame on a regular Cartesian grid with incorporation of metrics of the applied Azimuthal Equidistant Projection (AEP) for mathematically rigorous compensation of distortions of the Earth spherical geometry [*Kulchitsky et al.,* 2005]. Specifications of neutral thermosphere (temperature, composition) as well as neutral winds normally are derived from MSIS and HWM empirical models respectively. As the latest advance under development, EPPIM can be combined with theoretical model NCAR TIGCM [Roble and Ridley, 1987] for specification of the neutral thermosphere parameters (temperature and winds) for certain applications, primarily the real-time operation. For such arrangements the TIGCM model is driven by the same set of inputs as the EPPIM and the 5º x 5º TIGCM output is interpolated to EPPIM high-resolution grid at each time step. All other necessary polar ionosphere inputs are present in the model either as the period-specific data, when available, or, in most cases, are derived from statistical or empirical modules. These statistical modules are governed by the major geophysical indices such as *Kp/Ap*, $F_{10.7}$, and the solar wind parameters. Important input of the magnetospheric electric field is derived from the empirical representation by Weimer [2001], which is continuously driven by the solar wind parameters. Selection of such driver is especially advantageous for forecasting operation of the EPPIM, when the model time is forward-shifted and the electric field derivation utilizes upstream measurements of the solar wind by ACE satellite. For its diagnostic runs the EPPIM can utilize the SuperDARN electric filed model as an input (http://superdarn.jhuapl.edu). This arrangement allows for taking advantage of the data-driven real-time augmentation of SuperDARN electric field model.

EPPIM covers region pole ward from 50ºN of the geomagnetic latitude. This selection of the side boundary minimizes occurrences of horizontal trans-boundary fluxes due to horizontal $\mathbf{E}\times\mathbf{B}$-drift in the polar ionosphere. The model upper boundary (in the current version, up to 1000 km) is comprised by the empirically adjusted plasma flux. At the model lower boundary (80 km), the ionospheric plasma is assumed to be in the photochemical equilibrium. To match performance of different computational platforms, the model horizontal resolution can be adjusted in a wide range from 100x100 km (a capability of the current mid-range notebook) to 10x10 km or better (Massive Parallel Processing supercomputer). Computational robustness of the model ranges from sustaining the real-time capability on slower platforms to processing of hundreds times faster than the real-time in the parallel computational environment. The later mode, when up to several model years can be computationally covered in a few calendar days allows for intensive past processing, model testing, empirical corrections, and massive statistical validation. Regular Eulerian grid and parallel numerical organization of the model facilitates its high-resolution performance and, consequently, gradient-resolving capabilities [*Kulchitsky et al.*, 2005].

3.0 UAF EPPIM REAL TIME OPERARTION

The EPPIM supports continuous real-time forecasting operation by utilizing automatic remote feed of geophysical inputs from the NOAA Space Environment Center and other on-line depositories. Among these inputs is the solar wind data, which is measured by ACE satellite at the upstream position at the first Lagrangian point. This gravity-free location is at the Sun-Earth axis, approximately 1.5 million kilometers from the Earth. The solar wind measurements are delivered to on-line users with remarkably short delay of only 2-3 minutes. This operation of the NOAA Deep Space Network facilitates short-term forecasting capabilities of the EPPIM. During its forecasting run, the EPPIM model time is dynamically forward-shifted by the solar wind propagation delay. This propagation delay depends on the solar wind speed and, on average, ranges in the 1.5-2 hours. On the output side (http://www.arsc.edu/SpaceWeather), the model generates a number of forecasting products, including the ionospheric maps, animations, real-time comparisons with ionosonde network, comparisons with the ionospheric tomography cross-sections, and others. For this run the model horizontal resolution was selected at 35x35 km, while the model upper boundary was set at 500 km with 10 km altitude step. The EPPIM time-dependent output is specified on this regular 3-D Eulerian grid. All results described in this paper were obtained during the EPPIM real-time run, performed in fully automatic mode.

During its real-time forecasting run, the EPPIM is undergoing statistical validation. Massive (>200,000 measurements/year) comparisons are performed with the ionosondes data from the NOAA SEC real-time network (see list in Figure 1) and from other facilities (for instance, HAARP digizonde at Gakona, Alaska).

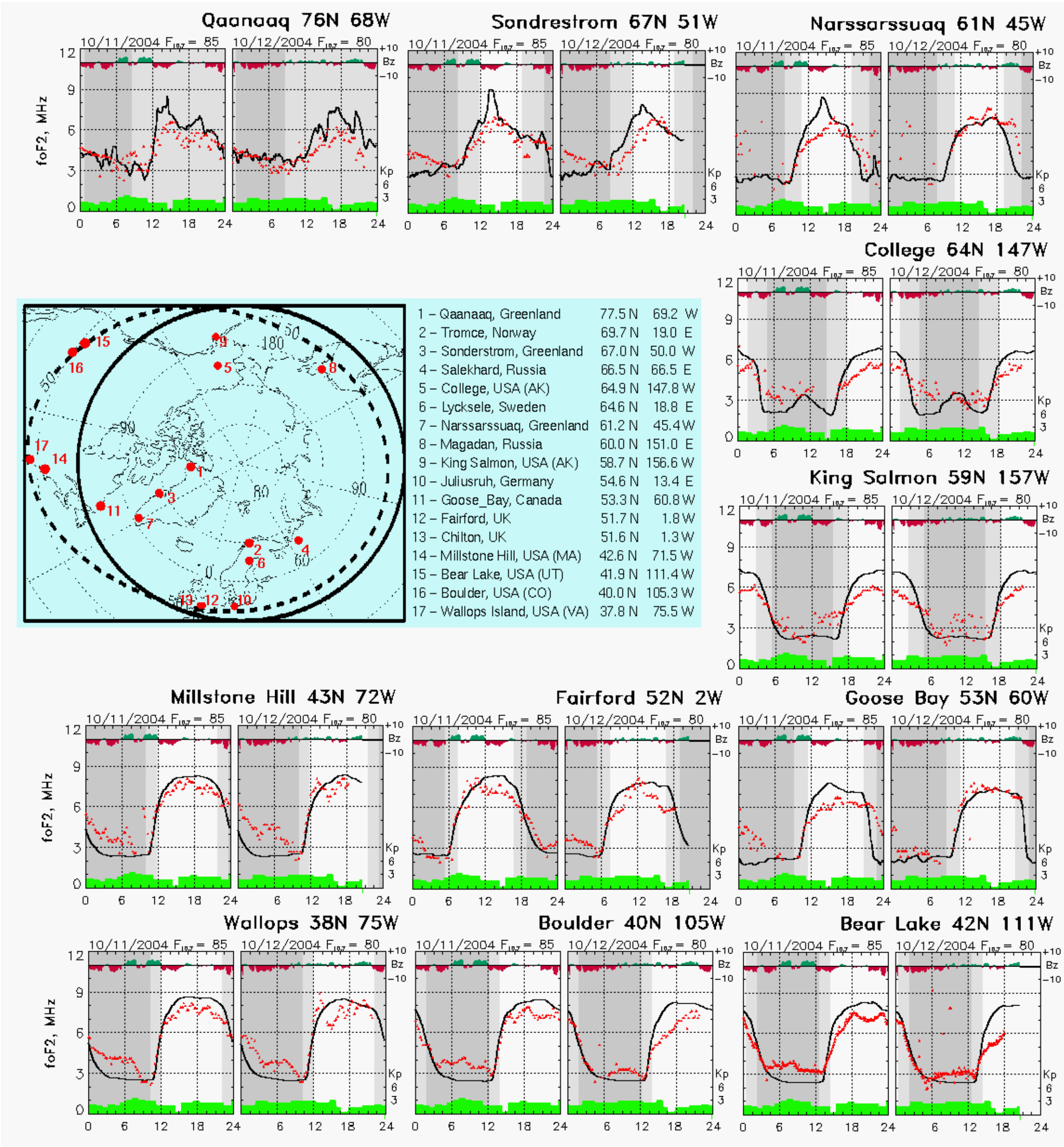

Figure 1: Locations of ionosondes from the NOAA Space Environment Center real-time network (http://sec.noaa.gov/ftpmenu/lists/iono_day.html) situated inside the UAF EPPIM simulation domain (geographic and geomagnetic latitudes of 50º*N* are shown as solid and dashed circles respectively). Two-day samples of comparisons of the model simulations (solid line) with the measured *foF2* (red triangles) are presented for different geophysical locations. Polar cap stations (Qanaaq, Sonderstrom) show strong modulation of *foF2* superimposed with diurnal trends, auroral stations (Narssarssuaq, College) indicate a presence of the auroral ionization, mid-latitude stations demonstrate pronounced daily trends. The time histories of geomagnetic activity and B_z–component of the IMF are shown on the plots, different background shades depict local daytime (white, zenith angle is less than 80º), night-time (dark gray, z. a. is more than 105º), and twilights (light gray, 80º < z. a. < 105º).

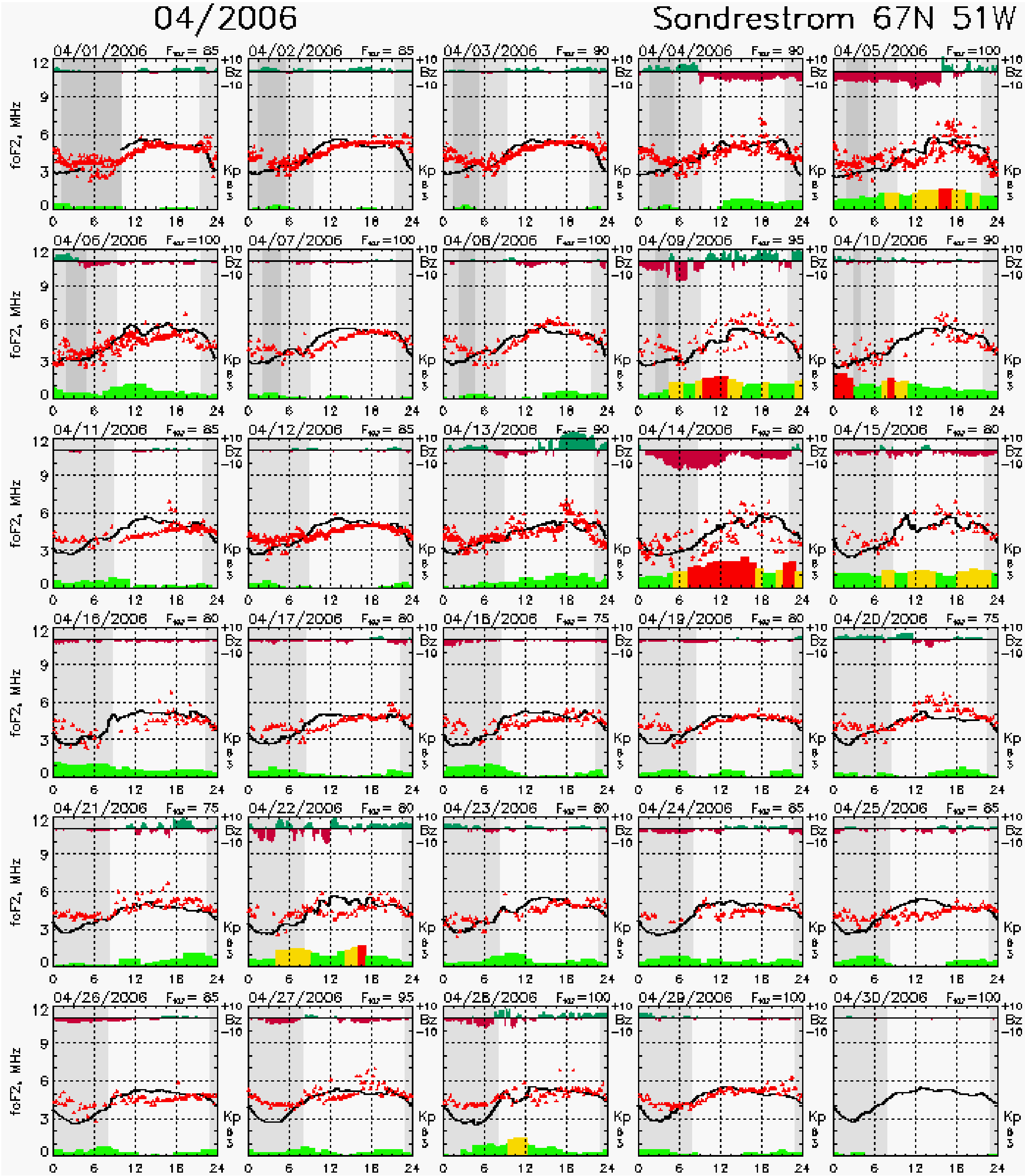

Figure 2a: An example of longer-term comparisons at Sondersrom polar cap location during geo-magnetically disturbed month of April, 2006. Superposition of diurnal trend and instantaneous modulation of the foF2 curve by passing ionospheric structures is typical for this location. The EPPIM simulations with statistical electric field model frequently capture the modulation range but do not follow trends on point-by-point manner. (See caption of Figure 1 for more on the plot details).

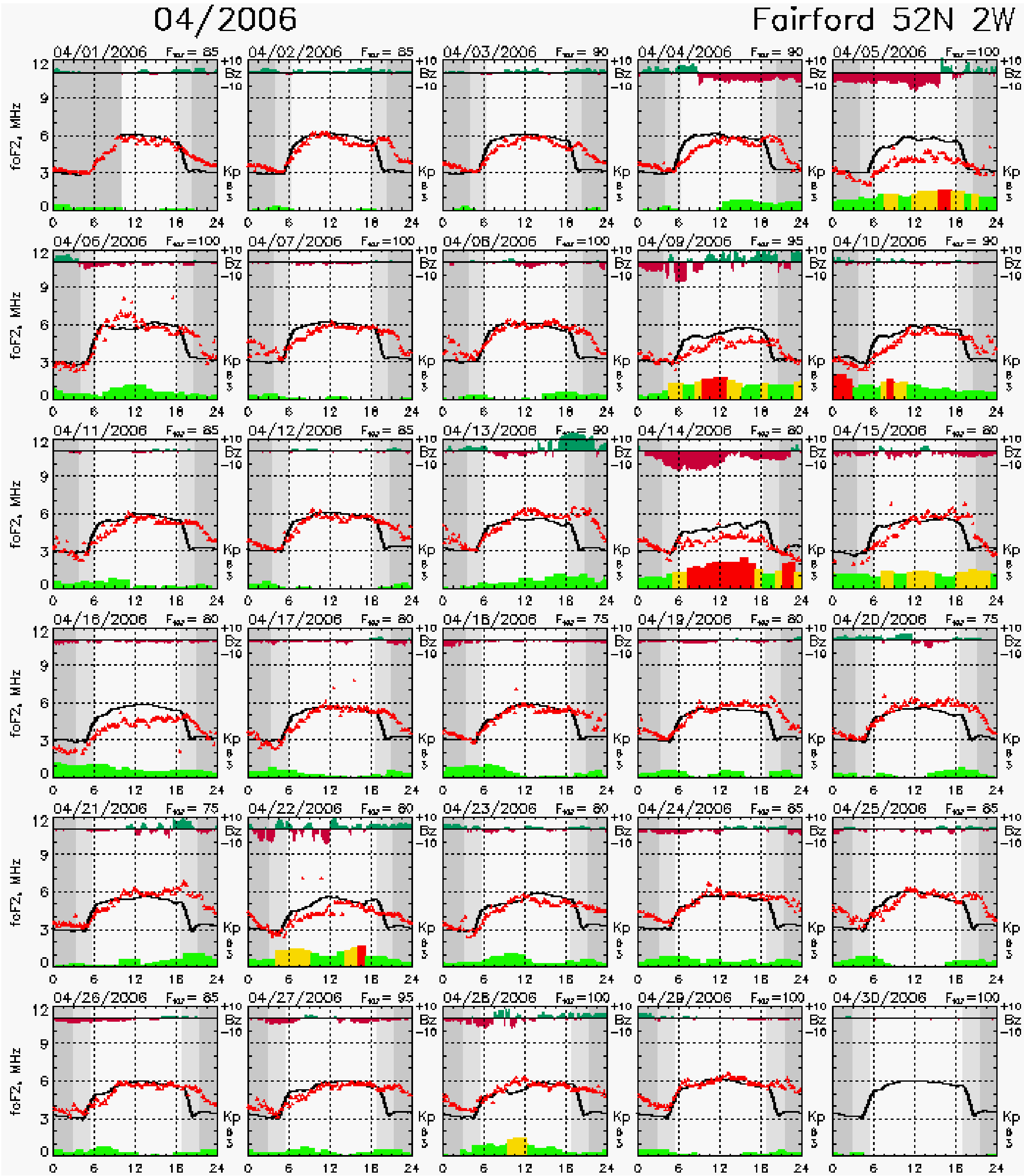

Figure 2b: Same period of comparisons as in Figure 2a, but for mid-latitude location of Fairford. Compared to the polar cap location of Sonderstrom, much smoother trends are prevailing at mid-latitudes. Generally, the agreement is noticeable better during geomagnetically quieter periods. The trends of the negative storm phase are not fully followed by the simulation (model "overshoots").

For this comparisons critical plasma frequency *foF2* of the main ionospheric peak at the F2-layer altitudes is emulated from 3-D distribution of the electron density using the following relation

$$foF2[MHz] = 8.98 \times 10^{-3} \sqrt{N_e^{\max}[cm^{-3}]}, \qquad (1)$$

where $N_e^{\max}[cm^{-3}]$ is the maximal electron density value in the 1-D vertical profile closest to the comparison ionosonde. All results in graphical and in tabular form are immediately published and archived at the EPPIM WWW-site. Two examples of the archived month-long daily comparisons are shown above in Figure 2a (comparisons with Sondersrom station, which is situated at the dynamic boundary of the polar cap and the auroral zone) and in Figure 2b (mid-latitude station Fairford in UK).

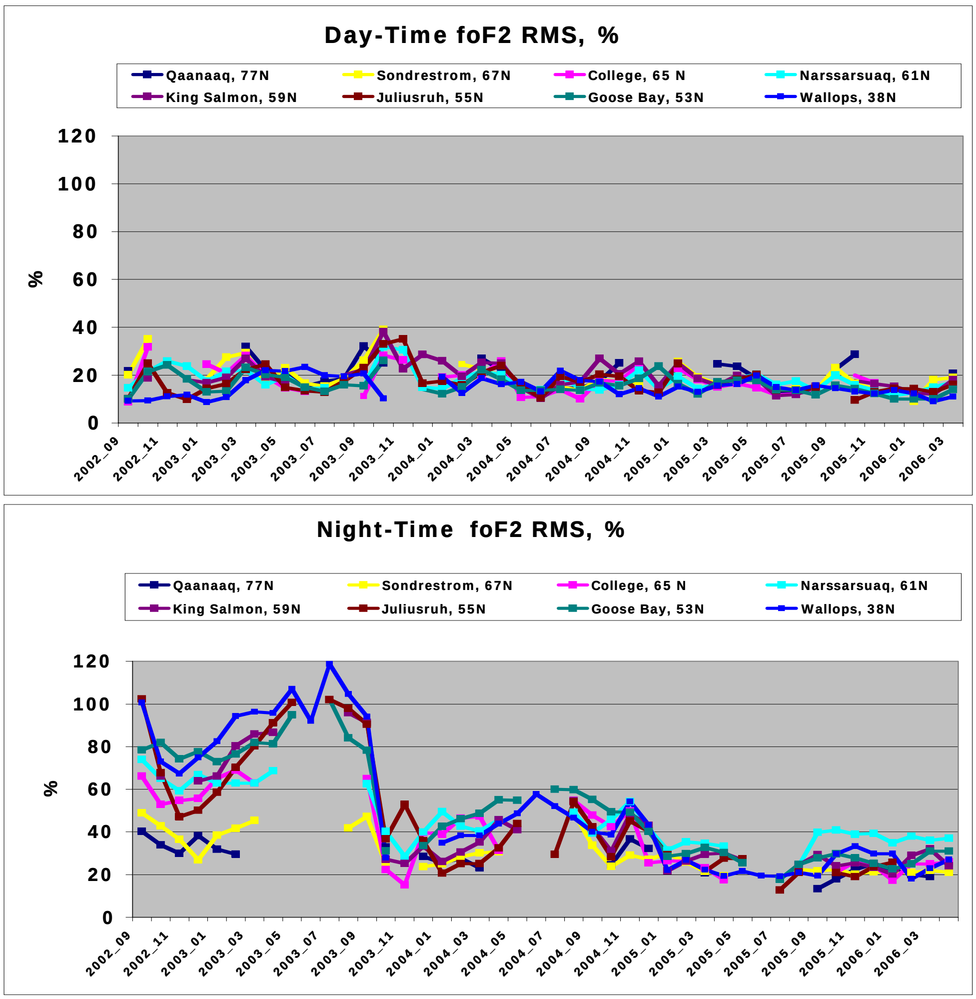

Figure 3: Long-term trends of the daytime and nighttime relative RMS of comparisons of the EPPIM-generated *foF2* with the ionosonde data from representative stations. Nighttime trend reflects consistent improvement of the agreement after two empirical corrections of the model (11/2003 and 1/2005). Both corrections (modifications of the upper boundary condition on the downward plasma flux) were aimed at minimization of the model statistical bias (see Figure 4).

Figure 3 shows the long-term trends of the monthly daytime and nighttime RMS for representative selection of ionospheric stations, obtained starting from the beginning of the model validation in 2002. The plot shows that typical daytime relative RMS of the emulated *foF2* forecast vs. measured data is in the 10-25% range depending somewhat on the latitude of the comparison station. This is especially true for the extreme high latitude locations of Qaanaaq and Sonderstrom, which typically exhibit somewhat higher RMS. Throughout the entire period of comparisons the range of daytime RMS demonstrates no major trends, except for a short spike in October-November of 2003. For these two months of exceptionally strong geomagnetic activity (Halloween Storm of 2003) the daytime RMS values are elevated by about 5-10%. This finding corresponds to the observed trend of the RMS as a function of geomagnetic activity, which will be discussed below in Section 4.

By contrast, the nighttime RMS exhibits significant trend during the period of observations of 2002 to 2006. This trend reflects two consequent improvements of the model introduced in November of 2003 and in January of 2005. Early results of 2002 and 2003 demonstrated significant and systematic disagreement with the measurements, characterized by both elevated RMS (up to 100% and even worse in Figure 3) and by the statistical bias, which essentially deviated from near-zero range during this initial period (Figure 4) to negative values of up to -100%. Both these factors indicate significant systematic underestimate of the nighttime electron densities by the inonospheric model at that time.

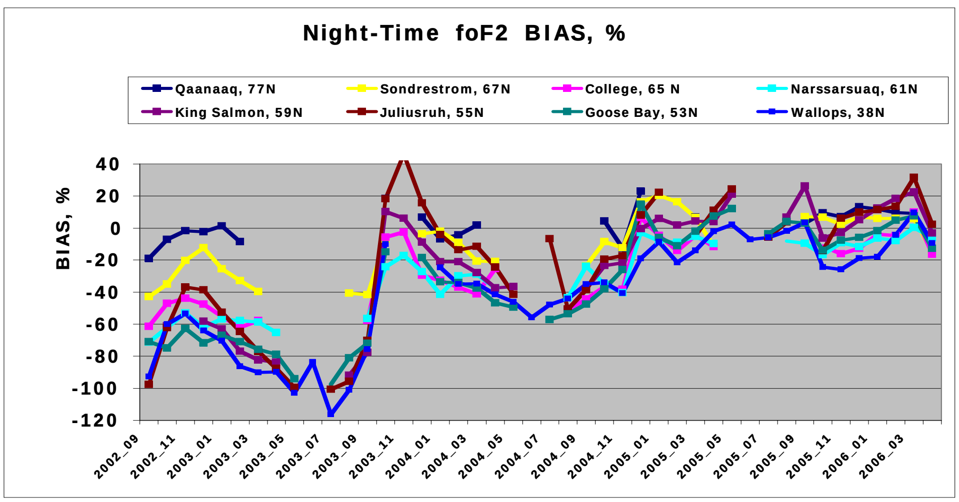

Figure 4: Long-term trend of the relative statistical bias of the nighttime *foF2* forecasting. First correction of the model nighttime parameters (11/2003) noticeably reduced the bias deviation from near-zero range. It took second comprehensive correction (1/2005) though to completely eliminate deterministic seasonal trend in the bias and restore the bias stochastic behavior. This is a reliable indicator that the EPPIM systematic errors are largely removed (see text).

In this study relative statistical bias of *foF2* was defined as the algebraic sum of "emulated vs. measured" individual deviations divided by the half-sum of emulated and measured values, which was averaged by the number of comparisons and transferred to percent (Equation 2). Note that division by the half-sum of the emulated and measured values was applied in this study for the relative RMS estimates as well (Equation 3). In the absence of systematic model errors mutual compensation of random discrepancies eliminates the bias, while a systematic model undershoot or overshoot results in the negative or positive bias respectively.

Regardless if bias is positive or negative, the corresponding systematic error contributes to the total RMS, increasing its systematic component additionally to the random one, which is always present (Equation 4).

$$BIAS[\%] = \frac{100\%}{N}\sum_{i=1}^{N}\frac{foF2_i^{\text{model}} - foF2_i^{\text{data}}}{\left(foF2_i^{\text{model}} + foF2_i^{\text{data}}\right)/2} \tag{2}$$

$$RMS[\%] = 100\%\sqrt{\frac{1}{N}\sum_{i=1}^{N}\left[\frac{foF2_i^{\text{model}} - foF2_i^{\text{data}}}{\left(foF2_i^{\text{model}} + foF2_i^{\text{data}}\right)/2}\right]^2} \tag{3}$$

$$RMS_{total} = \sqrt{RMS_{systematic}^2 + RMS_{random}^2} \tag{4}$$

From the RMS minimization standpoint, its purely random component is a measure of inherent variability of the stochastic processes, which usually is either impossible or very difficult to modify. For instance, noticeable reduction of the ionospheric forecasting random error can be achieved by dramatic improvement of the inputs quality, which is the field-advancing task of paramount complexity. By contrast, the RMS systematic component frequently can be eliminated without such significant efforts. Returning to the ionospheric modeling, usually it takes the model correction to totally eliminate or even reduce the systematic discrepancies. Thus, monitoring of statistical bias is a convenient way to establish a need for such correction.

In the EPPIM case, early comparisons reveal the model tendency at the time to underestimate nighttime electron density and, consequently, the emulated critical frequency. This underestimation had latitudinal dependence and seasonal trends, quite obvious on the 2002-2003 part of the nighttime plots of RMS and statistical bias on Figures 3 and 4. For instance, the extreme high-latitude locations of Sondersrom amd, especially, Qaanaq demonstrated the lowest RMS practically without any explicit seasonal trend and close to zero bias. In the same time, for the mid-latitude stations elevated RMS with pronounced seasonal trend were typical as well as a strongly negative bias. A tendency for relative increase of RMS while the station latitude decreases was quite obvious, which was also true for bias departure form zero. The worst results both in terms of high RMS and negative bias up to -100% (model undershoot by factor of 2) were obtained at Wallops Island ionosonde station, which is situated at 37°N of geographic latitude. Upon collection of statistical information on discrepancies during the first year of comparisons, an empirical correction on the upper boundary condition was introduced for compensation of the model low prediction. This compensation was achieved by introducing the latitudinal and seasonal dependences to the nighttime downward plasma flux through the model upper boundary.

It is well established that the nighttime ionospheric density is maintained by influx of plasma along the closed magnetic field line, which originates at the geomagnetically conjugated point in the sunlit hemisphere. This physical mechanism does not affect high-latitude locations in the open field lines zone (which one more time was demonstrated by our findings on the RMS and statistical bias trends for the high-latitude Qaanaaq and Sonderstrom). The flux has the order of magnitude of ~10^8 [$cm^{-2}sec^{-1}$], which is quite sufficient to change the ionization/recombination balance of the nighttime ionosphere. In the same time, as an outflux at the day-side this magnitude is not large enough to modify noticeably the daytime ionospheric parameters. The flux magnitude depends on the electron density gradient along the magnetic tube between the dark and sunlit hemispheres, which introduces latitudinal and seasonal dependence. For non-global ionospheric model such as EPPIM, the deterministic modeling of such dependence is not feasible and instead the empirical correction must be undertaken.

This empirical correction of the EPPIM was done first time upon collection of statistical information on biases of the uncorrected model during period of September of 2002 to October of 2003. The period of observation of the entire year allowed for taking into full account the seasonal dependence. Correction was constructed in a way that inside the zone of closed magnetic field lines the nighttime downward fluxes were adjusted according to the season and geomagnetic location such as the statistical bias was minimized as much as it was possible using collected information. The first correction was introduced in November of 2003 and noticeably improved the model nighttime predictions as Figure 3 clearly indicates. However, some residual biases were still present in the model, which is visible in Figure 3 as a seasonal trend of the RMS errors during the second year of observation (November 2003 to December 2004). It took full second year for collection of additional information to facilitate an improvement of analytical representation for the empirical correction. Particularly helpful was information from the mid-latitude stations newly included at that period into the real-time network (Fairford, UK; Chilton, UK; Boulder, CO; and Bear Lake, UT). This improved second correction was introduced in January of 2005 and finally eliminated the residual biases, including seasonal trends. It reduced the current level of nighttime RMS to the range of 20% to 40%. Currently, the statistical analysis demonstrates that the model biases (both the nighttime and the daytime once) are reasonably close to zero, which is indicative of successful minimization of the model systematic discrepancies. Hence, the daytime and nighttime RMS values discussed above are mainly characteristics of the residual random error of the adopted in EPPIM forecasting scheme. This scheme in a time-dependent manner adopts inputs for the ionospheric simulation, which are driven, in turn, by the period-specific distribution of the geophysical drivers through statistical (or "climatological") models. It is instructive to explore geophysical dependencies of the collected RMS in terms of the geomagnetic activity and variations of the solar wind parameters.

4.0 GEOMAGNETIC ACTIVITY DEPENDENCE OF THE FORECASTING RMS.

It is a well known phenomenon in geophysical research that geomagnetically undisturbed or just moderately disturbed days are strongly prevailing by shear numbers over disturbed periods, leave alone strong magnetic storms which statistically represent just a few percent of all days in the 11 year cycle of the solar activity. With certain reservations, the same is true for the solar activity. This is reflected in the level of validity of statistical geophysical models, which EPPIM uses as inputs for the forecasts. Much more information available for the quieter periods yields the better models of undisturbed conditions. Part of the problem is that the disturbances demonstrate more case-to-case variability and inherently are more difficult to describe in the statistical terms. Deficiencies of the statistical models for taking into account a prior history of the geophysical situation is also well known. For instance, post-storm variability of the $[O]/[N_2]$ ratio is not adequately described by the statistical models of neutral thermosphere such as MSIS. As any ionospheric model, EPPIM heavily relies on this parameter in its photochemical scheme and is highly sensitive to its value. Needless to add, simplifications of the ionospheric model itself are more likely to be more pronounced for simulation of geophysically disturbed situations. At any rate, it was expected that the EPPIM forecasting results for less disturbed periods should demonstrate higher accuracy.

For this study, all comparison data were loaded to the database. Results of parsing this database with inquiries on dependence of the RMS on the geomagnetic activity level are shown on Figure 5. To eliminate possible influence of other important factors, the dependencies are binned for groups "Daytime: winter, equinox, summer" and "Nighttime: winter, equinox". Here the season was defined by the calendar month and to distinguish "daytime" vs. "nighttime" the zenith angle was taken into consideration. "Daytime" was defined as periods with zenith angles less than 85º and "nighttime" was defined by zenith angles exceeding 105º. (This definition practically eliminated category "Nighttime: Summer" from the consideration since only a few mid-latitude locations can supply comparisons data, which can meet this criteria. Because of small number of points for averaging, their statistical validity is rather low.) Figure 5 shows these dependencies and demonstrates that forecasting accuracy degradation with increase of the geomagnetic activity although exists

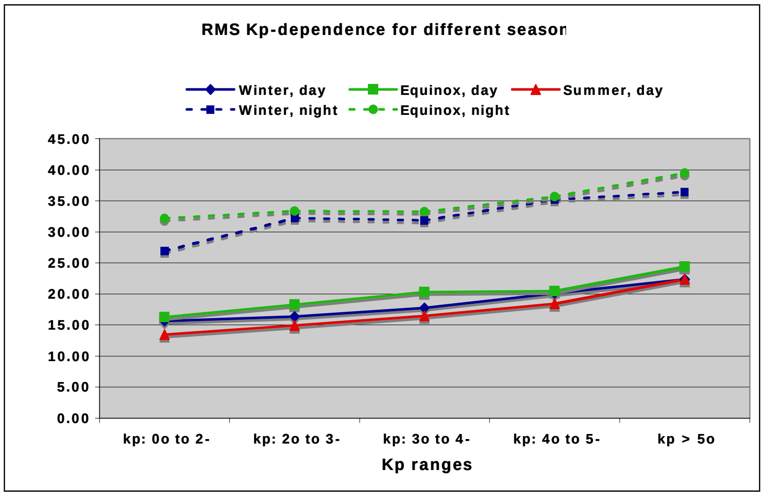

Figure 5: Dependencies of the relative forecasting RMS on geomagnetic activity for various seasons and times of the day. General tendency is a degradation of the forecasting accuracy and increase of the RMS by 8-10% during transition from quite conditions (Kp = 0o to 2o) to disturbed conditions (Kp exceeds 5o). This tendency is remarkably uniform for all times of the day and different seasons.

but it is not particularly large. Overall gain in RMS is about 8-10% for transition from quite geomagnetic activity levels of Kp = 0o to 2o to disturbed conditions of Kp exceeding 5o. This increase is pretty uniform for all times of the day and for different seasons.

Figure 5 also shows interesting dependencies of RMS averaged over large array of data. Compared to rather noisy trends shown in Figure 3, where RMS are separated for particular stations, averaging of data in Figure 5 allows for filtering out this noise. It makes possible to specify long-term average RMS for particular season and geomagnetic activity level without nuances of geographic (or, for that matter, geomagnetic) location of particular stations. Such specification for the daytime indicates that overall RMS varies from 15% at the low and moderate geomagnetic activity to 20% for moderately disturbed levels (Kp = 4o to 5o), and increases to just under 25% for the disturbed periods (Kp exceeds 5o). Seasonal dependence, if it really exists, is rather small in the 2-5% range. Some increase (by 2% or so) of the winter RMS with respect to the summer one is pretty persistent, while the equinox comparisons yield another 2-3% increase compared to the wintertime. Similar figures for the nighttime RMS are 25-30%, 30-35%, and up to 40% for the low, moderate, and disturbed geomagnetic activity conditions respectively. Similarly to the daytime findings, slight increase by about 2% for the equinox nighttime RMS compared to the winter RMS is observed. Concluding this discussion, it worth to point out that the total number of comparisons generalized in Figure 5 was just under 500,000, or approximately 100,000 per curve, or, neglecting comparative overrepresentation of the low Kp cases, 20,000 per each point on the curves. Such massive and long-term averaging makes uncertainties in determination of average RMS rather small and permits to conclude that the established numbers are statistically confident with a high probability. Apparently, this is the reason that there is practically no visible noise in the comparisons results in Figure 5.

5.0 CONCLUSIONS AND FUTURE WORK

This research determines statistically prevailing errors for the high- and mid-latitude real-time ionospheric modeling with the theoretical ionospheric model UAF EPPIM. The high-resolution model was applied to short-term forecasting of elements of the space weather using for simulations statistical inputs driven, in turn, by the period-specific distribution of the major geophysical indices. The forecasting WWW-site is operational at the ARSC for several years (http://www.arsc.edu/SpaceWeather) and presently available for the users of various forecasting products. It was found by massive (~200,000 a year) statistical comparison with ionosonde measurements that the typical daytime error of the *foF2* forecast is in 10-15% to 20-25% range, depending on the level of geomagnetic activity and season. Similar nighttime results are in the 20-35% to 30-40% range respectively. It was shown that control of the statistical bias is a useful mean to identify and to eliminate systematic errors in the model. Outcome of such elimination was discussed on example of empirical correction of the nighttime EPPIM predictions.

These conclusions can have impact on the following future studies using UAF EPPIM and, perhaps, other models. Determination of the baseline forecasting errors for theoretical modeling besides its own interest is a necessary step for monitoring of the model development in terms of impact on the prevailing forecasting accuracy. This is generally true also for application of various data assimilation schemes (Kalman filtering, for instance) for the post-simulation correction of the output. The problem is especially acute in the polar latitudes, where data sources are sparse and their coverage is frequently irregular. In this condition the data-assimilative correction is prone to rely heavily on a single data source often without possibility to weight its statistical influence by other means. Tight monitoring of the output accuracy dynamics is a way to mitigate a possibility of such undesirable scenario.

Sparse coverage of the ionospheric data-producing facilities in the polar region attracts special interest to the limited list of available resources. If in the mid-latitudes the number one real-time ionospheric data source is slant TEC parameter massively collected using GPS satellites signals and disseminated on-line by the COORS network, in the polar region the NOAA SEC real-time ionosonde network is significant additional resource. Experience working with that resource on-line is a positive asset of the EPPIM program, which will be applied for future studies. Future research plans for the EPPIM-based Space Weather forecasting operation includes data-driven correction of the outputs using ionosonde data. Monitoring of possible improvement of the forecasting accuracy is a part of this future study.

ACKNOWLEDGEMENTS

This work was supported in part by a grant of HPC resources from the Arctic Region Supercomputing Center (ARSC) at the University of Alaska Fairbanks (UAF) as part of the Department of Defence High Performance Computing Modernization Program. Authors acknowledge valuable contribution of the ARSC Research Assistants Larisa Stoltzfus and Chris Hikushi to managing and handling the comparisons database.

REFERENCES

Kulchitsky, A., S. A. Maurits, B. J. Watkins, and J. McAllister. (2005), **E** x **B** Drift Simulation in an Eulerian Ionospheric Model Using the TVD Numerical Scheme, *J. Geophys. Res., 110,* A09310, doi: 10. 1029/2005JA011033.

Maurits, S.A., and B. J. Watkins. (1996), UAF Eulerian Model of the Polar Ionosphere, in Solar Terrestrial Energy Program (STEP): *Handbook of Ionospheric Models*, edited by R. W. Schunk, pp. 95-123, Utah State University.

Maurits, S.A., J. McAllister, and B.Watkins, WWW-based Visualization of the Real-Time Run of a Space Weather Forecast, Proceedings of Eurograph-IEEEE Visualization Symposium' 2000, May 2000, Amsterdam, Springer-Verlag, 2000.

Roble, R.G., E.C. Ridley, An auroral model for the NCAR thermospheric general corculation model (TGCM), *Ann. Geophys, ser. A*, 5, No.6, 369-382, 1987.

Schunk, R.W., L. Scherliess, J. J. Sojka, D. C. Thompson, L. Zhu, D. N. Anderson, M. Codrescu, C. Minter, T. J. Fuller-Rowell, R. A. Heelis, M. Hairston, B.M. Howe, Global Assimilation of Ionospheric Measurements (GAIM), (2004), Radio Science, vol. 39, RS1S02, doi: 10. 1029/2002RS002794.

Wang, C., G. Hajj, X.Pi, I.G. Rosen, and B.Wilson (2004), Development of the Global Assimilative Ionospheric Model, *Radio Sci., 39*, RS1S06, doi: 10.1029/2002RS002854.

Weimer, D. R. (2001), An improved model of ionospheric electric potential including substorm perturbation and application to the Geospace Environment Modeling November 24, 19996 event. *J.Geophys. Res*., *106*, 407.